miR-375 upregulates lipid metabolism and inhibits cell proliferation involved in chicken fatty liver formation and inheritance via targeting recombination signal binding protein for immunoglobulin kappa J region (*RBPJ*)

Yong-Hong Zhang,[*,1] Heng-Li Xie,[*,1] Yu-Wei Yang,[*] Jie Wen,[†] Ran-Ran Liu,[†] Gui-Ping Zhao,[†] Xiao-Dong Tan,[†] Zhen Liu,[†] Yi Zheng,[†] and Jia-Bao Zhang[*,2]

[*]*College of Animal Science, Jilin University, Changchun 130062, P. R. China; and* [†]*Institute of Animal Sciences, Chinese Academy of Agricultural Sciences, Beijing 100193, P.R. China*

ABSTRACT Poultry is susceptible to fatty liver which lead to decrease egg production and increase mortality. But the potential molecular mechanisms remain largely unclear. In the current study, in combination with transcriptome sequencing and miRNA sequencing data analysis from F1 generation of the normal liver and fatty liver tissues, the differentially expressed *miR-375* and its target gene *RBPJ* were screened and verified. The expression levels of *miR-375* and *RBPJ* gene in the liver between control and fatty liver groups of F0-F3 generation for Jingxing-Huang (**JXH**) chicken are different significantly ($P < 0.05$ or $P < 0.01$). And downregulated *RBPJ* expression can promote TG content and lipid droplets in primary hepatocytes cultured in vitro ($P < 0.01$). Cell proliferation-related genes, including *PMP22, IGF-1, IGF-2*, and *IGFBP-5,* increased or decreased significantly after overexpression or knockdown *RBPJ* ($P < 0.05$ or $P < 0.01$), respectively. This study uniquely revealed that *miR-375* induced lipid synthesis and inhibited cell proliferation may partly due to regulation of *RBPJ* expression, thereby involving in fatty liver formation and inheritance in chicken. The results could be useful in identifying candidate genes and revealing the pathogenesis of fatty liver that may be used for disease-resistance selective breeding in chicken.

Key words: chicken, fatty liver, *miR-375*, *RBPJ*, lipid metabolism

2023 Poultry Science 102:102218
https://doi.org/10.1016/j.psj.2022.102218

INTRODUCTION

Unlike mammals, the liver is the main organ for lipid synthesis in poultry. Abnormal liver fatty acid oxidation, lipoprotein transport, or fat synthesis will cause excessive accumulation of fat in the liver, thereby inducing fatty liver (Burdge and Lillycrop, 2014). Fatty liver is a metabolic disease (Lewis and Mohanty, 2010), which is more common in laying hens(Zhang et al., 2018). Although the fatality rate induced by fatty liver is low (Clark and Diehl, 2003), but it affects the chicken's performance such as egg production, fertilization rate, and hatchability rate (Zhang et al., 2018).

Non-coding RNAs including miRNA are important transcription regulators in physiological and pathological processes (Sayed and Abdellatif, 2011; Hulsmans et al., 2011; Huang et al., 2014). More and more researches have been focused on the role of miRNA in the development of related diseases. Recent study demonstrates that miRNA has an important effect on liver lipid metabolism in poultry (Marques-Rocha et al., 2015). Some studies have shown that in the development of nonalcoholic fatty liver, some tissue specific miRNA may play a key role in regulating the post transcriptional regulation of the key process of liver injury related to this disease (Panera et al., 2014). A study of 47 patients with nonalcoholic fatty liver showed that the expression levels of *miR-122, miR-192*, and *miR-375* are significantly upregulated, and the upregulation levels are related to the severity of the disease (Pirola et al., 2015). Auguet et al. (2016) found that the expression of *miR-33* in liver tissue and blood of nonalcoholic fatty liver disease (**NAFLD**) patients is also upregulated, and upregulated *miR-33* can prevent obesity and liver steatosis in mice (Price et al., 2018). The expression of *miR-34a* is related to their susceptibility to NAFLD based on the study for mice fed a high-fat diet (Pogribny et al., 2010). Inhibiting the expression of *miR-34a* in obese

Received November 2, 2021.
Accepted September 29, 2022.

[1]These authors contributed equally to the work and share the first author.

[2]Corresponding author: zjb@jlu.edu.cn

mice can change the expression of related metabolic genes and metabolic results (Fu et al., 2012). Studies for the NAFLD patients found that the expression of *miR-34a* in the serum is upregulated (Cermelli et al., 2011; Yamada et al., 2013; Liu et al., 2016; Salvoza et al., 2016), and the upregulated level is related to the severity of the disease (Castro et al., 2013). In short, miRNAs could affect liver lipid metabolism and the occurrence of nonalcoholic fatty liver disease by regulating target genes in related pathways (Butler, 1976; Burdge and Lillycrop, 2014; Ferreira et al., 2014; Huang and Hu, 2015; Rozenboim et al., 2016; Ansen-Wilson and Lipinski, 2017; McCarty, 2017).

In the present study, the F1 generation from the chicken fatty liver model induced by high-fat and low-protein diets was used (Zhang et al., 2018). In combination with transcriptome and miRNA sequencing data analysis for F1 generation of the control and fatty liver groups, the differential expression miRNAs and targeted genes were screened, and verified between control and fatty liver group of F0−F3 generation for Jingxing-Huang (**JXH**) chicken. At the same time, the regulation to lipid metabolism for the differential expression miRNA and its targeted gene was also studied in primary hepatocytes cultured in vitro. This study will provide a valuable resource to reveal the formation and inheritance of fatty liver. The results could be useful in identifying candidate genes for fatty liver that could be used for disease-resistance selective breeding in chicken.

MATERIALS AND METHODS

Ethics Approval

All the animal experiments were conducted in accordance with the guidelines for experimental animals established by the Ministry of Science and Technology, Beijing, China. Ethical approval on animal survival was given by the animal ethics committee of the Institute of Animal Sciences, Chinese Academy of Agricultural Sciences, Beijing, China (**IASCAAS-AE**-03).

Sample Collection

The **JXH** chickens of F0 generation for the fatty liver were induced by a high-fat diet, but the chickens for the control group were fed basal diet, as reported by Zhang (Zhang et al., 2018). The offspring of the F1, F2, and F3 generations were produced by male **JXH** chickens without (control group) or with (fatty liver group) fatty liver. All the F1, F2, and F3 generations in two groups were fed a basal diet. The time for liver collection from F0 to F3 generation was at the end of the 36th wk. And the liver tissues for miRNA sequencing of F1 generation including the control group and fatty liver group were the same as Xiaodong Tan et al. (2021).

miRNA Sequencing and DE miRNA Analysis

After the sample passed the test, the Small RNA Sample Pre-Kit was used to construct the library (Novogene, Beijing). Using the special structures of the 3′ and 5′ ends of small RNA (the 5′ end has a complete phosphate group and the 3′ end has a hydroxyl group), with total RNA as the starting sample, the 2 ends of small RNA were directly spliced, and then the reverse transcription was used to synthesize cDNA. After PCR amplification, the target DNA fragment was separated by PAGE gel electrophoresis, and the cDNA library was recovered by cutting gel. The libraries were constructed and sequenced on the Illumina HiSeq2000 platform (Illumina, San Diego, CA) in a single lane.

When the sample has biological duplication, the default screening condition of differential miRNA is: $P < 0.05$. In order to control the false positive rate, we need q-value combined with foldchange to screen. The default screening condition is: q-value < 0.01 & $|\log2(\text{foldchange})| > 1$.

KEGG Enrichment Analysis

KEGG (Kyoto Encyclopedia of Genes and Genomes, http://www.kegg.jp/) was a database of whole genome and metabolic pathway. Each pathway in KEGG was enriched through hypergeometric test, and the *P*-value was corrected by multiple tests with $q < 0.05$ as the threshold. The pathways satisfying this condition were defined as those significantly enriched from target genes of differentially expressed miRNAs. Here, KEGG enrichment was measured by rich factor, Q-value and the number of genes enriched in this pathway. Rich factor refers to the ratio of the number for differentially expressed genes to the total number of annotated genes in the pathway entry. The larger the rich factor, the greater the degree of enrichment. Q-value is the *P*-value corrected by multiple hypothesis tests. The value range of Q-value is [0,1]. The closer to zero, the more significant the enrichment. And the first 30 enriched path entries were selected to display in this figure. If the number of enriched path entries is less than 30, all of them will be displayed.

GO Enrichment Analysis

GO (Gene Ontology, http://geneontology.org/) was used for function annotation of target genes of differentially expressed miRNA. According to the number of differentially expressed genes contained in each GO term, hypergeometric test was used to find out the significantly enriched GO term compared with the whole genome background. GO term with $q < 0.05$ was selected as the highly enriched GO term for target genes. The main biological functions of targets of differentially expressed miRNAs could be determined by go enrichment analysis. This method is based on Wallenius non-central hyper-geometric distribution. Compared with the general Hyper-geometric distribution, the

distribution is characterized by that the probability of extracting individuals from a certain category is different from that of extracting an individual from a certain category. The difference of this probability is obtained by estimating the preference of gene length, so that the probability of GO term being enriched by candidate target gene can be calculated more accurately.

Target Prediction and Luciferase Assay

Base on the miRNA sequencing result, significantly differentially expressed (**DE**) miRNAs were selected for subsequent studies. In addition, combined with GO and KEGG analysis, we focused on the role of *miR-375* in fatty liver. As well as, we chose the target genes of *miR-375* via predicting software TargetScan (http://www.targetscan.org/vert_72/). Importantly, in our previous research, we found *RBPJ* is a key DE gene in inherited phenotype of acquired fatty liver in chicken. In addition, *RBPJ* may be an important gene related to chicken fatty liver (Tan et al., 2021). Therefore, we speculate that *miR-375* may regulate fatty liver through *RBPJ*.

Then, 3′UTR fragment (wild type and mutation) of *RBPJ* were cloned into luciferase assay vectors, respectively. *miR-375* mimic co-transfected with wild-*RBPJ*-3′UTR and mutate-*RBPJ*-3′UTR into cells. The luciferase assay refers to Dual Luciferase Reporter Gene Assay Kit (Roche, Basel, Switzerland).

qRT-PCR

β-actin and *U6* were used as house-keeping gene for mRNA and miRNA detection, respectively, and the gene expression levels of *miR-375, RBPJ, PMP22, IGF-1, IGF-2*, and *IGFBP-5* were detected. Primers used for qRT-PCR were designed using the Primer 5.0 software. All primers were synthesized by Sangon Biotech Co., Ltd. (Shanghai, China) and listed in Table 1. Trizol reagent (ThermoFisher SCIENTIFIC, Shanghai) was used to extract total RNA from liver tissues and primary hepatocytes cultured in vitro. The mRNA expression levels were detected in triplicate using the SYBR Green Ⅰ dye. The qRT-PCR mixture consisted of cDNA (1 μL), PCR-Master Mix (5 μL), PCR-F-Primer (0.5 μL), PCR-R-Primer (0.5 μL), and RNase-free H_2O (3 μL) in a total volume of 10 μL. The reaction conditions were as follows: 95°C denaturation for 1 min, followed by 40 cycles of denaturation at 95°C for 15 s, annealing at 60°C for 15 s, and extension at 72°C for 15 s. The data obtained from the Eppendorf qRT-PCR instrument (Hamburg, Germany) were analyzed using the $2^{-\triangle\triangle CT}$ method.

Primary Hepatocytes Isolated and Cultured In Vitro

After sterilizing the 15-d embryonic embryos, opened the abdominal cavity and isolated the liver, soak them in PBS containing double antibodies for 3 times, and put them into 1 mL 0.25% Collagenase Type Ⅱ lyophilized (ThermoFisher SCIENTIFIC, 17101015), then ground the liver tissue mass until there was no obvious tissue mass, digested them at 37°C, 5% CO_2 incubator for 25 min, then added 0.5 mL trypsin for 10 min. Filter the cell suspension through a 70-μm cell sieve, added DMEM/F-12 (DF-12, Biological Industries) with Fetal Bovine Serum (**FBS**, Chenghe) to terminate the digestion, centrifuge at 800 g/min for 5 min, discarded the supernatant, then seeded into 6-well plates with the cell density of $10^6 \cdot mL^{-1}$, incubated at 37°C.

miR-375 mimic NC, miR-375 mimic, miR-375 Inhibitor Transfection

Primary hepatocytes cells were plated two days before transfection at density of approximately 1×10^6 cells/

Table 1. The genes and related primers for qRT-PCR.

Gene	Primer sequence (5'-3')	Annealing temperature (°C)	Product size (bp)
U6	RT: CGCTTCACGAATTTGCGTGTCAT	/	/
miR-375	RT:CTCAACTGGTGTCGTGGAGTCGGCAATTCAGTTGAGTAA	/	/
miR-375	F:ACACTCCAGCTGGGTTTGTTCGTTCGGCTC R:CTCAAGTGTGGAGTCGGCAA	60	72
U6	F:GCTTCGGCACATATACTAAAAT R:CGCTTCACGAATTTGCGTGTCAT	60	80
RBPJ	F: CATACACACCGGAACCAGGG R: TGGTTGGATTTGGGCTGACA	73	60
β-actin	F:GAGAAATTGTGCGTGACATCA R: CCTGAACCTCTCATTGCCA	60	152
PMP22	F: TCTTCGTCTCCACCATCGTCA R:GTGAAGAGCTGGCAGAAGAACAG	60	208
IGF-1	F: AGAAGCCGTTGTGCGAGAA R: GCACTCAGGATGGCAACACTC	60	143
IGF-2	F: TGTGGAGGAGTGCTGCTTTC R: GGGAGGTGGCGGAGAGGTCA	60	98
IGFBP-5	F: CCTCTCTGACCTCAAAGCTGA R: ACCATCCTCTGGCTGCTCT	60	198

Abbreviations: *IGF-1*, insulin-like growth factor-1; *IGF-2*, insulin-like growth factor-2; *IGFBP-5*, insulin-like growth factor binding protein-5; *PMP22*, peripheral myelin protein 22; *RBPJ*, recombination signal binding protein for immunoglobulin kappa J region.

well into 6-well culture plates. miR-375 mimic NC and miR-375 inhibitor NC served as the control for miR-375 mimic and miR-375 inhibitor, respectively. All transfection sequences were transfected at a final concentration of 150 nM by use of Lipofectamine 2000 (ThermoFisher SCIENTIFIC, Waltham, MA). After 48 h transfection, the cells were used to extract total RNA. Each transfection was performed in triplicate, and three independent experiments were conducted.

siRBPJ and RBPJ Overexpression Plasmid Transfection

After the primary hepatocytes isolated in vitro were cultured for 48 h, the medium was changed to DF-12, and then *siRBPJ* and *RBPJ* plasmids (the final concentration is 5 μg) were added with 3 μL Lipofectamine 2000 (ThermoFisher SCIENTIFIC). Then the cells were cultured 48 h for subsequent detection.

Triglyceride Content Detection

After hepatocytes were cultured and transfected with *miR-375* mimic NC, *miR-375* mimic, *miR-375* inhibitor, *siRBPJ*, and *RBPJ* overexpression plasmids for 48 h, triglyceride (**TG**) content was measured by triglyceride (TG) enzymatic method Test kit E1013 (APPLYGEN, Beijing) separately.

Oil Red O Staining

To explore the role of *miR-375* and *RBPJ* on lipid formation, after *miR-375* mimic NC, *miR-375* mimic, *miR-375* inhibitor, *siRBPJ*, and *RBPJ* overexpression plasmids transfection for 48 h, the hepatocytes were stained with Oil Red O detection kit (Solarbio LIFE SCIENCE, Beijing).

Data Analysis

The data were presented as the means ± S.D. All data represent 3 independent experiments. Two-sided Student's t test was used to calculate P-values. Significance is displayed as $^{*}P \leq 0.05$ or $^{**}P \leq 0.01$.

RESUILS

Different Expressed miRNA Analysis in Liver Tissue

After removal of low-quality and adaptor containing reads, the clean reads were aligned to the swine reference sequences by Bowtie (setting allows one mismatch) and the distribution and coverage of reads on reference genes were calculated (Table 2). We identified that 26 miRNAs were significantly differentially expressed (DE) (Table 3), in which 14 miRNAs (gga-miR-375, gga-miR-1a-3p and gga-miR-2188-3p et al.) were upregulated and 12 miRNAs (gga-miR-222a, gga-miR-221-3p, and gga-miR-155 et al.) were downregulated in fatty liver group, respectively. Among these, miR-375 was chosen for further analysis based on having the most significant fold change and highly expressed DE one in fatty liver group.

Table 2. The quality of the data.

Sample	Reads	Error rate	Q20	Q30	GC content
C_miR1	14438306	0.01%	99.29%	98.09%	48.97%
C_miR2	17474283	0.01%	99.60%	98.80%	49.21%
C_miR3	15108013	0.01%	99.57%	98.82%	48.62%
C_miR4	15384176	0.01%	99.74%	99.30%	50.15%
FL_miR1	13501813	0.01%	99.61%	98.85%	49.57%
FL_miR2	14973300	0.01%	99.57%	98.75%	49.31%
FL_miR3	13141504	0.01%	99.51%	98.66%	50.34%
FL_miR4	13188263	0.01%	99.58%	98.86%	50.65%

Abbreviations: C, control group; FL, fatty liver group.

Next, target genes of *miR-375* were used to performed in KEGG pathway enrichment and GO analysis to unravel the miRNA-mediated biological processes associated with development of fatty liver. In the results of KEGG enrichment analysis, the target genes targeted by *miR-375* are involved in many related pathways. For example, the signaling pathways related to cellular processes mainly include regulation of Notch signaling, MAPK signaling, and glycerolipid metabolism pathways include fatty acid elongation, Citrate cycle (TCA cycle) and so on (Figure 1).

In GO enrichment analysis, the biological process involves in pathways that the target gene targeted by *miR-375* are mainly participate in positive regulation of cell proliferation and cell activation. Cellular component participates in cytoplasm, intracellular part. And the molecular function related to fatty-acyl-COA binding and carbohydrate derivative binding pathways (Figure 2).

Target Gene Prediction and Validation of miR-375

In order to prove the targeting relationship between *miR-375* and gene *RBPJ*, the binding site was analyzed (Figure 3A) with the software TargetScan (http://www.targetscan.org/vert_72/), and result indicated that *miR-375* can target binding *RBPJ*. To investigate the potential targeting of *RBPJ* by *miR-375*, luciferase activity assay was used. The *RBPJ*-3′UTR-luciferase reporter plasmid and reporter plasmid with mutated 3′UTR sequence (**Mut**) were constructed (Figure 3B). The result shown that *miR-375* inhibit the luciferase activity of the *RBPJ*-3′UTR reporter ($P < 0.01$), instead of the Mut reporter with the altered sequence ($P > 0.05$; Figure 3B). Together, these data suggest that *miR-375* may affect the expression of *RBPJ* by targeting the *RBPJ*-3′UTR.

In order to prove the regulation of *miR-375* on its targeted genes, the *RBPJ* express levels were detected after transfecting *miR-375* mimic NC, *miR-375* mimic, *miR-375* inhibitor NC, and *miR-375* inhibitor for 48 h in primary hepatocytes cultured in vitro. The results showed that compared with NC group, the expression of *miR-375* was significantly upregulated after *miR-375* mimic

Table 3. Differentially expressed miRNAs.

		Fatty liver group Readcount					Control group Readcount							
FL vs. C	miRNA	FL_miR1	FL_miR2	FL_miR3	FL_miR4	FL_miR	C_miR1	C_miR2	C_miR3	C_miR4	C_miR	log2Fold Change	*P* val	*P* adj
Upregulated	gga-miR-375	1,881	6,773	3,012	7,679	4959.130	3,131	863	1,342	1,510	1445.541	1.489	3.7E-05	1.5E-03
	gga-miR-1a-3p	948	4178	7,427	3,525	4115.490	5,802	1,278	515	1,576	1493.984	1.149	4.1E-03	9.2E-02
	gga-miR-2188-3p	8	7	6	3	7.065	4	1	1	2	1.529	1.213	1.2E-02	NA
	gga-miR-22-3p	3,523	5,004	5,333	3,027	4659.707	6,672	2,974	1,866	3,564	3018.232	0.586	1.5E-02	1.9E-01
	gga-miR-219a	219	357	425	397	377.494	698	272	128	241	249.206	0.559	1.7E-02	1.9E-01
	gga-miR-219b	219	357	425	397	377.494	698	272	128	241	249.206	0.559	1.7E-02	1.9E-01
	gga-miR-140-5p	874	1,224	1,133	1,108	1194.478	1,366	902	490	1,065	809.884	0.529	2.1E-02	2.1E-01
	gga-miR-144-3p	317	96	237	26	217.417	62	81	50	90	67.695	1.055	2.5E-02	2.4E-01
	gga-miR-12229-3p	15	10	1	10	11.033	10	3	1	2	2.677	1.056	3.0E-02	NA
	gga-miR-143-5p	379	755	873	303	619.551	533	381	251	434	352.990	0.707	3.3E-02	2.6E-01
	gga-miR-1729-5p	61	146	242	48	131.209	98	67	44	83	63.869	0.832	3.5E-02	NA
	gga-miR-24-5p	10	4	12	8	10.091	5	2	2	7	3.370	0.986	3.6E-02	NA
	novel_210	14	165	50	9	56.032	74	3	7	26	17.064	0.980	4.2E-02	NA
	gga-miR-216b	2	3	1	4	2.736	1	0	0	1	0.316	0.937	4.7E-02	NA
	gga-miR-222a	192	599	352	236	357.419	3,576	825	354	1,969	1155.489	−1.444	3.0E-05	1.5E-03
Downregulated	gga-miR-221-3p	336	760	632	389	562.367	3,399	1,115	534	1,891	1272.032	−1.085	3.9E-05	1.5E-03
	gga-miR-155	40	136	68	86	84.915	355	133	88	517	217.990	−1.112	3.1E-03	8.7E-02
	gga-miR-34c-5p	1	2	18	5	6.814	48	15	48	40	37.916	−1.414	3.2E-03	NA
	gga-miR-221-5p	123	298	299	136	226.077	867	371	217	589	403.732	−0.759	6.9E-03	1.3E-01
	novel_194	1	0	1	0	0.666	11	6	1	8	4.813	−1.244	1.1E-02	NA
	gga-miR-130b-5p	29	96	30	71	58.197	295	123	48	131	110.891	−0.811	1.2E-02	NA
	gga-miR-222b-5p	0	2	1	3	1.456	12	5	2	21	7.820	−1.193	1.4E-02	NA
	gga-miR-223	77	193	186	137	155.919	439	274	144	297	240.919	−0.579	1.7E-02	1.9E-01
	gga-miR-130a-5p	4	15	7	12	9.715	48	48	22	8	28.519	−1.056	1.8E-02	NA
	gga-miR-363-5p	2	10	6	8	6.554	40	10	7	25	15.052	−0.903	2.9E-02	NA
	gga-miR-9-5p	114	291	192	320	240.309	1558	211	211	598	435.119	−0.738	3.0E-02	2.6E-01

Abbreviations: C, control group; FL, fatty liver group.

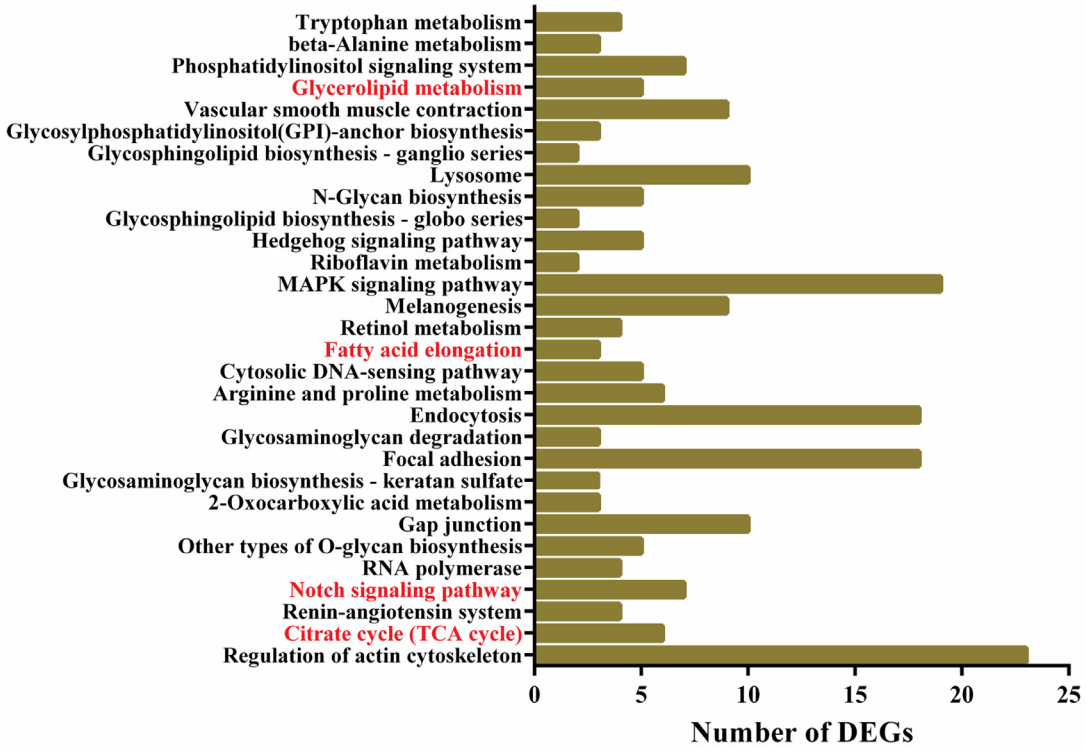

Figure 1. The histogram of candidate target genes involved KEGG pathway. Histogram of candidate target genes involved KEGG pathway, where the vertical axis represents pathway name, the horizontal axis represents the number of candidate target genes in this pathway.

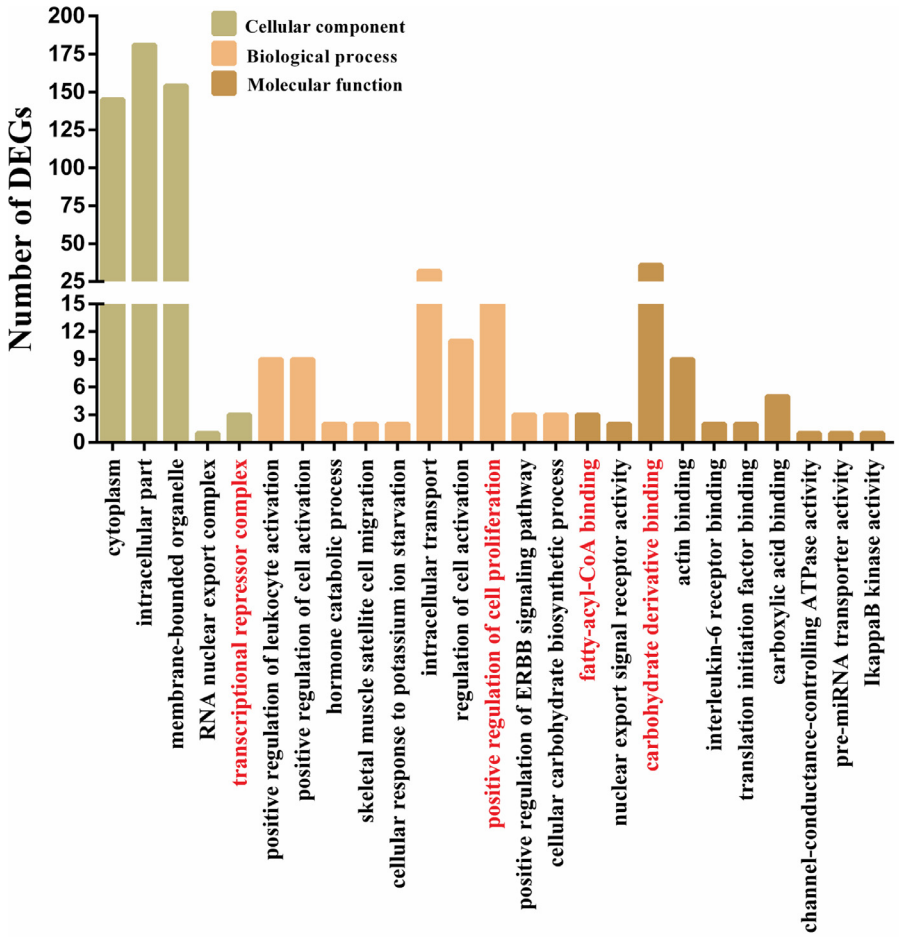

Figure 2. The histogram of GO enrichment of candidate target genes. The histogram of GO enrichment of candidate target genes. The horizontal axis is GO term of the next level in the three major categories of GO, and the vertical axis is the number of candidate target genes annotated to this term (including sub-terms of this term) and the proportion of the number of candidate target genes in the total number of annotated candidate target genes. The three different classifications represent the three basic classifications of GO term (from left to right, cell components, biological processes, and molecular functions).

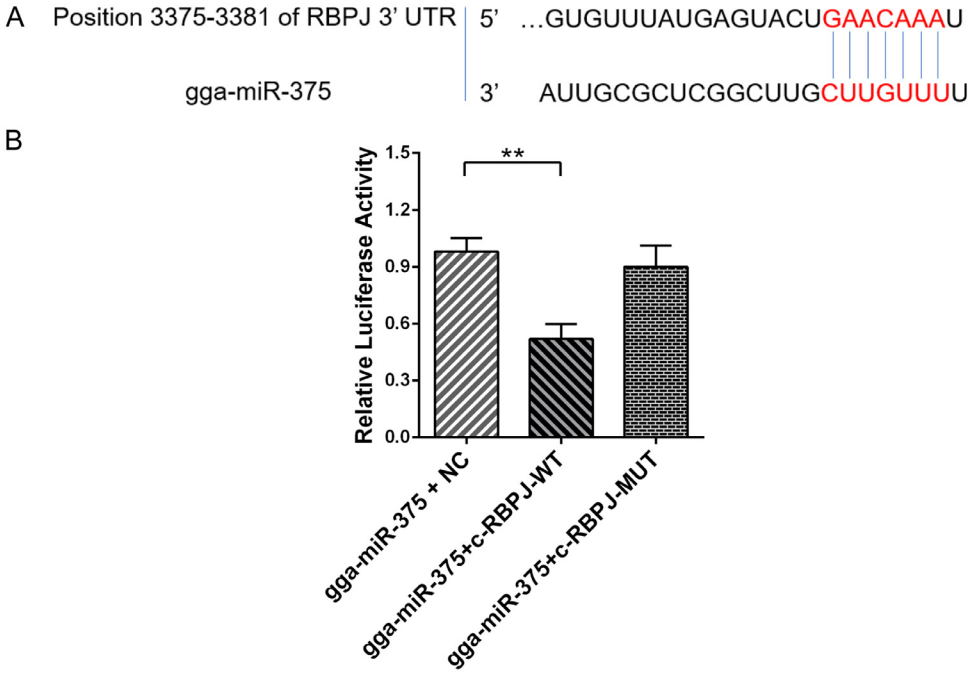

Figure 3. Targeting validation of miR-375 and RBPJ. Targeting validation of *miR-375* and *RBPJ*. (A) *miR-375* and *RBPJ* targeted binding sites predicted by software TargetScan (http://www.targetscan.org/vert_72/). (B) Dual luciferase reporter assay results for gga-*miR-375*+NC, the gga-*miR-375*+wild-type *RBPJ* and gga-*miR-375*+ mutant *RBPJ* groups. ** indicates $P \leq 0.01$. Abbreviation: *RBPJ*, recombination signal binding protein for immunoglobulin kappa J region.

transfection ($P < 0.01$) and downregulated after *miR-375* inhibitor transfection ($P < 0.05$). In addition, the expression levels of *RBPJ* have significant downregulated ($P < 0.001$) or upregulated ($P < 0.001$) after *miR-375* mimic or *miR-375* inhibitor transfection compared with the NC group, respectively (Figures 4A and 4B).

The Expression Levels of miR-375 and RBPJ in Liver Tissues Among Different Generations

To further verify the relationship of *miR-375* and *RBPJ* with fatty liver formation and inheritance, the

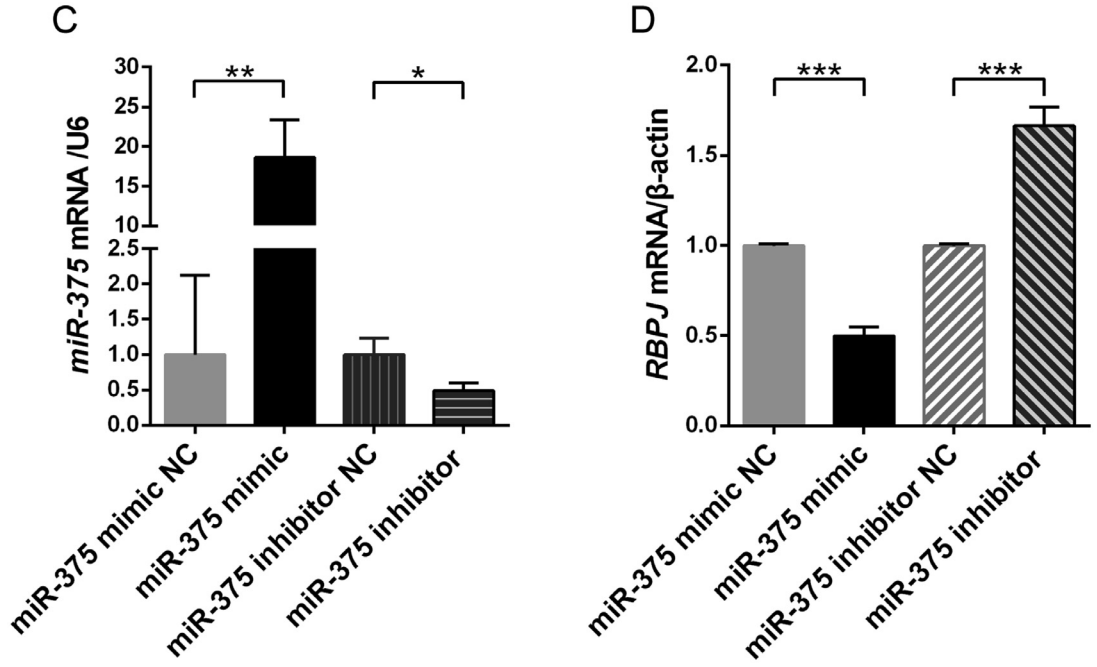

Figure 4. Expression level of genes in different groups of chicken primary hepatocytes. Expression level of genes in different groups of chicken primary hepatocytes. In (A and B), qRT-PCR was used to indicate the expression of *miR-375* and *RBPJ* in *miR-375* mimic NC, *miR-375* mimic, *miR-375* inhibitor NC and *miR-375* expression levels in the inhibitor group. * Indicates $P \leq 0.05$, ** indicates $P \leq 0.01$ and *** indicates $P \leq 0.001$. Abbreviation: *RBPJ*, recombination signal binding protein for immunoglobulin kappa J region.

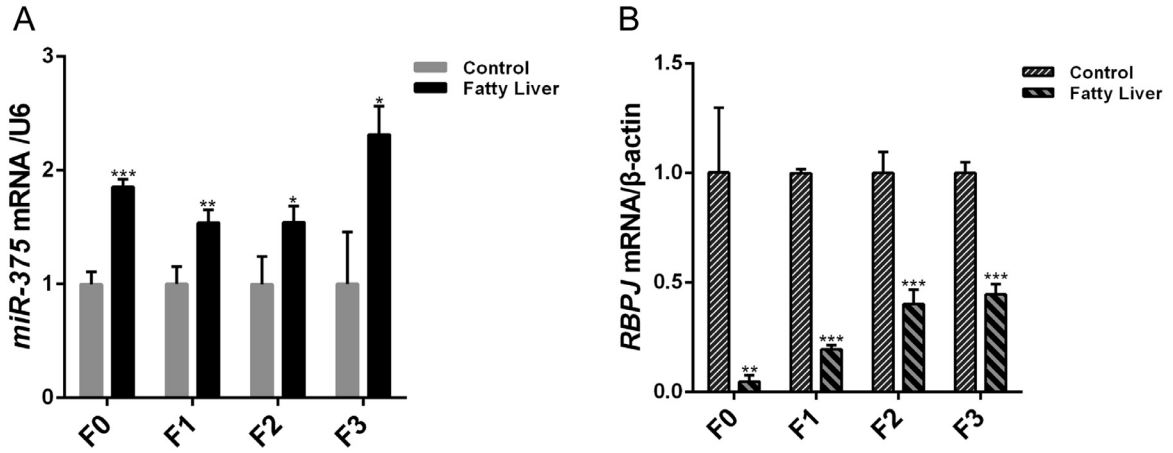

Figure 5. Expression level of miR-375 and RBPJ in normal liver and fatty liver from F0 to F3 generation. Expression level of *miR-375* and *RBPJ* in normal liver and fatty liver groups from F0 to F3 generation. (A and B) represent expression levels of *miR-375* and *RBPJ*, respectively, in control groups and fatty liver groups from F0 to F3 generation. * Indicates $P \leq 0.05$, ** indicates $P \leq 0.01$ and *** indicates $P \leq 0.001$. Abbreviation: *RBPJ*, recombination signal binding protein for immunoglobulin kappa J region.

expressions of *miR-375* and *RBPJ* were detected between the control group and fatty liver group from F0 to F3 generation in liver tissue of Jingxing-Huang (**JXH**) chickens by qRT-PCR. The results shown that *miR-375* have significantly higher expression in fatty liver groups from F0 to F3 generation ($P < 0.05$, $P < 0.01$, or $P < 0.001$) compared with control groups (Figure 5A). But the expression levels of *RBPJ* have the opposite trend from F0 to F3 generation ($P < 0.01$ or $P < 0.001$; Figure 5B). Therefore, we conduct that *miR-375* may play important role during fatty liver formation and inheritance depending on *RBPJ* in chicken.

The Triglyceride Content and Lipid Droplets Deposition in Primary Hepatocytes Cultured In Vitro

After transfection of *siRBPJ* and *RBPJ* plasmids, the *RBPJ* expression levels were significantly downregulated ($P < 0.01$) and upregulated ($P < 0.01$) respectively compared with NC group in primary hepatocytes cultured in vitro (Figure 6A).

The triglyceride content is significantly upregulated ($P < 0.01$ or $P < 0.05$) after *siRBPJ* or *miR-375* mimic transfection. While over-expressed *RBPJ* or inhibited *miR-375*, the triglyceride content is significantly downregulated compared with the NC group ($P < 0.01$; Figures 6B and 6C). In addition, the lipid droplets increased significantly when the expression of *RBPJ* was knocked down in primary hepatocytes cultured in vitro, while the lipid droplets decreased after the gene *RBPJ* was overexpressed compared with the NC group. And the lipid droplets in *miR-375* mimic or inhibitor transfection group were the same as knocked down or overexpressed *RBPJ* group (Figure 6D). Therefore, we concluded that *miR-375* may regulate triglycerides formation and lipid metabolism by targeting *RBPJ* gene.

Cell Proliferation Related Genes Detection in Primary Hepatocytes Cultured In Vitro

The expression levels of cell proliferation related genes including *PMP22, IGF-1, IGF-2*, and *IGFBP-5* were detected in primary hepatocytes cultured in vitro. The results shown that overexpression or knock-down of *RBPJ* could upregulate or downregulate the levels of *PMP22* ($P < 0.05$), *IGF-1* ($P < 0.05$), *IGF-2* ($P < 0.05$), and *IGFBP-5* ($P < 0.05$; Figures 7A−7D). Collectively, our findings demonstrate that *RBPJ* has an impact on hepatocyte proliferation.

DISCUSSION

The fatty liver is a metabolic disease caused by lipid metabolism disorder such as lipid absorption, lipid synthesis, β-oxidation, or lipoprotein transport (Adams et al., 2005). Fatty liver disease can further develop into nonalcoholic hepatitis, liver cirrhosis and hepatocellular carcinoma induced by nutritional, environmental, and genetic factors (Friedman et al., 2018), and negative impact on human health and animal production.

Fatty liver disease includes different stages of liver injury, from early steatosis or nonalcoholic fatty liver disease to nonalcoholic steatohepatitis related liver fibrosis (Brea and Puzo, 2013) regulated by related genes and signaling pathways. Researches shown that Notch signaling in collaboration with other tumor-promoting signaling pathways, including p53/Snail/IKKalpha/FOXA2/NUMB, induces liver cancer (Strazzabosco and Fabris, 2012; Zhou et al., 2012). And also, RBPJ-mediated Notch signaling regulates cell differentiation and plasticity in cooperation with other pathways (Hayward et al., 2008; Kopan and Ilagan, 2009). At present, the researches on *RBPJ* mainly focuses on the mechanism to HCC, and little research has done to the occurrence and genetics of fatty liver in

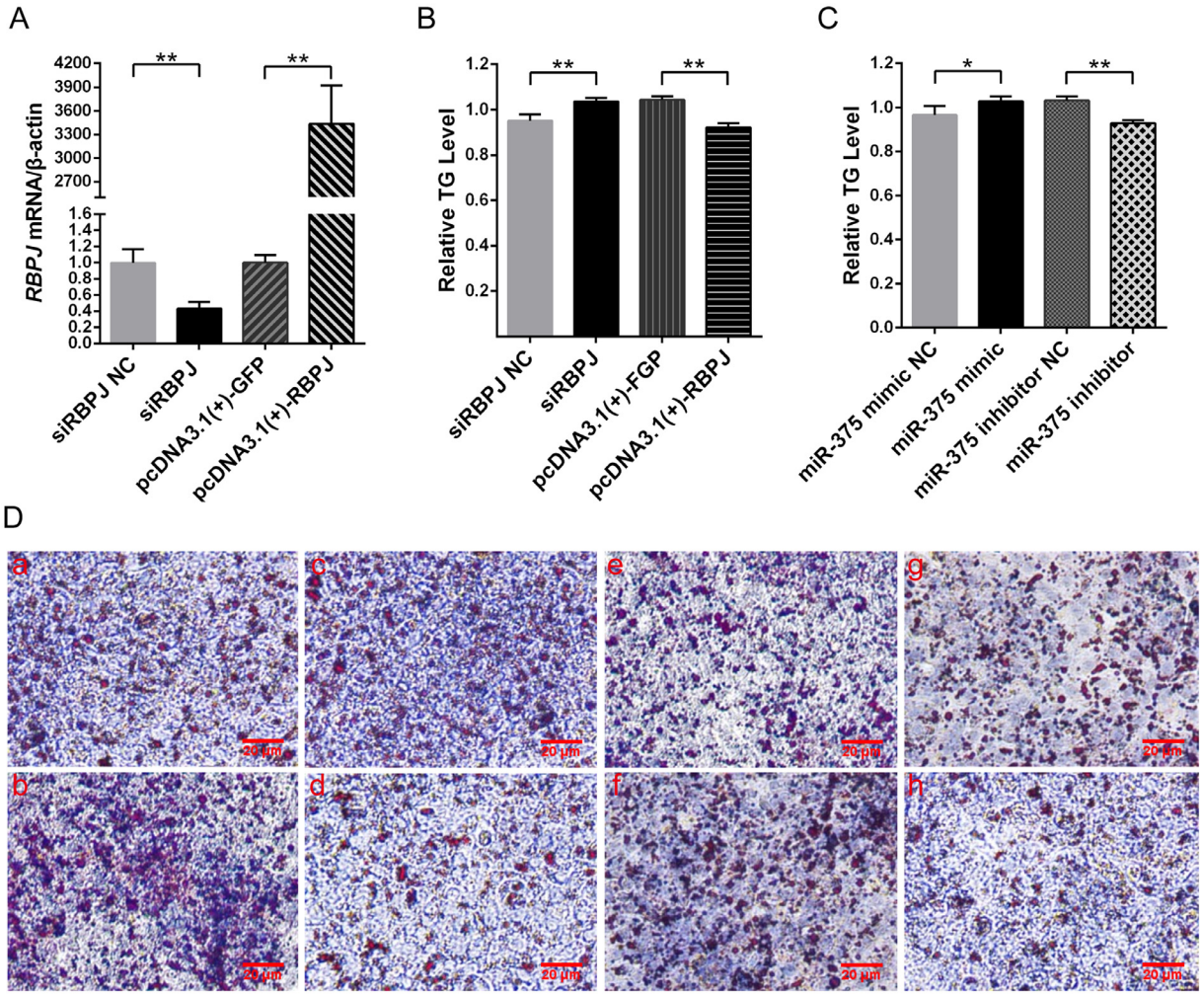

Figure 6. Gene expression levels, TG content and Oil red O staining in different groups. Gene expression levels, TG content and Oil red O staining in different groups. (A and B) represent *RBPJ* expression levels and TG content in *siRBPJ* NC, *siRBPJ*, pcDNA3.1 (+) -GFP and pcDNA3.1 (+) -*RBPJ* groups. (C) represents TG content in *miR-375* mimic NC, *miR-375* mimic, *miR-375* inhibitor NC, *miR-375* inhibitor group. (D) shows lipid droplets in different transfected groups, a represents *siRBPJ* NC group, b represents *siRBPJ* group, c represents pcDNA3.1 (+) -GFP group, d represents pcDNA3.1 (+) -*RBPJ* group, e represents *miR-375* mimic NC group, f represents *miR-375* mimic group, g represents *miR-375* inhibitor NC group, h represents *miR-375* inhibitor group. * Indicates $P \leq 0.05$ and ** indicates $P \leq 0.01$.

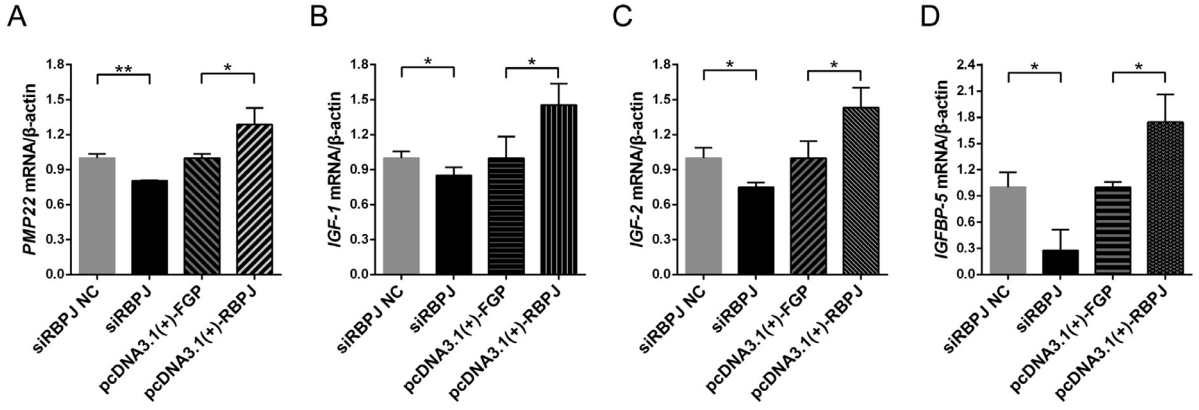

Figure 7. Cell proliferation related genes detection in primary hepatocytes cultured in vitro. Relative expression analysis results of cell proliferation related genes in different groups. (A−D) represent relative expression analysis results of *PMP22, IGF-1, IGF-2*, and *IGFBP-5* in *siRBPJ* NC, *siRBPJ*, pcDNA3.1 (+) -GFP and pcDNA3.1 (+) -*RBPJ* groups, respectively. * Indicates $P \leq 0.05$ and ** indicates $P \leq 0.01$. Abbreviations: *PMP22*, peripheral myelin protein 22; *IGF-1*, insulin-like growth factor-1; *IGF-2*, insulin-like growth factor-2; *IGFBP-5*, insulin-like growth factor binding protein-5.

chicken. In the present study, we found that the expression levels of *RBPJ* in the liver of fat liver groups from F0 to F3 generation higher than those of control groups ($P < 0.05$ or $P < 0.01$), at the same time, we found that triglyceride content and lipid droplets increased or decreased when *RBPJ* was knocked down or overexpressed in primary hepatocytes cultured in vitro, respectively. So, we deduce that *RBPJ* could regulate hepatic lipid metabolism involved in occurrence and genetics of fatty liver in chicken.

Researches also shown that *RBPJ* can promote cell proliferation during HCC occurrence (Kopan and Ilagan, 2009), whether *RBPJ* has the same impact on cell proliferation in fatty liver is uncertain. In this study, we found that cell proliferation-related genes, including *PMP22* (Hou et al., 2020), *IGF-1, IGF-2*, and *IGFBP-5* (Lang et al., 2006; Aguiar et al., 2013; Jiao et al., 2013) were increased or decreased significantly after overexpression or knock-down *RBPJ* ($P < 0.05$ or $P < 0.01$), respectively. The results indicate that *RBPJ* could also promote cell proliferation in primary hepatocytes cultured in vitro. But the expression levels of *RBPJ* in fat liver groups were decreased compare with those in control groups, and cell proliferation was inhibited during fat liver in chicken. So, the other reason for formation and inheritance of fat liver, we speculate, is that cell proliferation was inhibited under the *RBPJ* regulation.

Increasing evidence points to pivotal roles for *miR-375* in regulating fat accumulation and carcinogenesis. It has been proved that the expression levels of *miR-375* in human hepatoma tissues and hepatoma cell lines were significantly lower than those in control groups (Li et al., 2018). Some studies shown that *miR-375* further regulates the proliferation and migration of stem cells by regulating the transcription level of *YAP*, and then affects the occurrence and development of hepatocellular carcinoma (Liu et al., 2010). Our study shown that *RBPJ* is target gene of *miR-375*, and the expression levels of *miR-375* were higher in fatty liver groups compare with those in control groups from F0 to F3 generation ($P < 0.05$ or $P < 0.01$), and we also found that *miR-375* could regulate triglycerides formation and lipid droplet deposition in primary hepatocytes cultured in vitro. These results indicate that *miR-375* has a potential role in hepatic lipid metabolism via targeting *RBPJ*.

CONCLUSIONS

This study uniquely revealed that *miR-375* could upregulated lipid synthesis and inhibited cell proliferation which may partly due to regulation of *RBPJ* expression, thereby involving in fatty liver formation and inheritance in chicken. Our findings will provide a valuable resource to insight into the regulation mechanism for the formation and inheritance of fatty liver with the point of epigenetics, and suggested that modulating *miR-375* or *RBPJ* differential expression may represent a potential therapeutic strategy for fatty liver disease that could be used for disease-resistance selective breeding in chicken.

ACKNOWLEDGMENTS

This research was supported by grants from the Natural Science Foundation of Jilin Province of China (20210101362JC).

Data availability statement: The data that support the findings of this study are available from the corresponding author upon reasonable request.

DISCLOSURES

The authors declare that they have no competing interests.

SUPPLEMENTARY MATERIALS

Supplementary material associated with this article can be found, in the online version, at doi:10.1016/j.psj.2022.102218.

REFERENCES

Adams, L. A., J. F. Lymp, J. St Sauver, S. O. Sanderson, K. D. Lindor, A. Feldstein, and P. Angulo. 2005. The natural history of nonalcoholic fatty liver disease: a population-based cohort study. Gastroenterology 129:113–121.

Aguiar, A. F., I. J. Vechetti-Júnior, R. W. Alves de Souza, E. P. Castan, R. C. Milanezi-Aguiar, C. R. Padovani, R. F. Carvalho, and M. D. P. Silva. 2013. Myogenin, MyoD and IGF-I regulate muscle mass but not fiber-type conversion during resistance training in rats. Int. J. Sports Med. 34:293–301.

Ansen-Wilson, L. J., and R. J. Lipinski. 2017. Gene-environment interactions in cortical interneuron development and dysfunction: a review of preclinical studies. Neurotoxicology 58:120–129.

Auguet, T., G. Aragonès, A. Berlanga, E. Guiu-Jurado, A. Martí, S. Martínez, F. Sabench, M. Hernández, C. Aguilar, J. J. Sirvent, D. Del Castillo, and C. Richart. 2016. miR33a/miR33b* and miR122 as possible contributors to hepatic lipid metabolism in obese women with nonalcoholic fatty liver disease. Int. J. Mol. Sci. 17:E1620.

Brea, A., and J. Puzo. 2013. Non-alcoholic fatty liver disease and cardiovascular risk. Int. J. Cardiol. 167:1109–1117.

Burdge, G. C., and K. A. Lillycrop. 2014. Fatty acids and epigenetics. Curr. Opin. Clin. Nutr. Metab. Care 17:156–161.

Butler, E. J. 1976. Fatty liver diseases in the domestic fowl—a review. Avian Pathol. 5:1–14.

Castro, R. E., D. M. S. Ferreira, M. B. Afonso, P. M. Borralho, M. V. Machado, H. Cortez-Pinto, and C. M. P. Rodrigues. 2013. miR-34a/SIRT1/p53 is suppressed by ursodeoxycholic acid in the rat liver and activated by disease severity in human non-alcoholic fatty liver disease. J. Hepatol. 58:119–125.

Cermelli, S., A. Ruggieri, J. A. Marrero, G. N. Ioannou, and L. Beretta. 2011. Circulating microRNAs in patients with chronic hepatitis C and non-alcoholic fatty liver disease. PLoS One 6: e23937.

Clark, J. M., and A. M. Diehl. 2003. Nonalcoholic fatty liver disease: an underrecognized cause of cryptogenic cirrhosis. JAMA 289:3000–3004.

Ferreira, D. M. S., A. L. Simão, C. M. P. Rodrigues, and R. E. Castro. 2014. Revisiting the metabolic syndrome and paving the way for microRNAs in non-alcoholic fatty liver disease. FEBS J. 281:2503–2524.

Friedman, S. L., B. A. Neuschwander-Tetri, M. Rinella, and A. J. Sanyal. 2018. Mechanisms of NAFLD development and therapeutic strategies. Nat. Med. 24:908–922.

Fu, T., S.-E. Choi, D.-H. Kim, S. Seok, K. M. Suino-Powell, H. E. Xu, and J. K. Kemper. 2012. Aberrantly elevated microRNA-34a in obesity attenuates hepatic responses to FGF19 by targeting a membrane coreceptor β-Klotho. Proc. Natl. Acad. Sci. U. S. A. 109:16137–16142.

Hayward, P., T. Kalmar, and A. M. Arias. 2008. Wnt/Notch signalling and information processing during development. Development 135:411–424.

Hou, J., H. Zhuo, X. Chen, J. Cheng, W. Zheng, M. Zhong, and J. Cai. 2020. MiR-139-5p negatively regulates PMP22 to repress cell proliferation by targeting the NF-κB signaling pathway in gastric cancer. Int. J. Biol. Sci. 16:1218–1229.

Huang, T., and F. B. Hu. 2015. Gene-environment interactions and obesity: recent developments and future directions. BMC Med Genomics 8(Suppl 1):S2.

Huang, Y., Y. Liu, L. Li, B. Su, L. Yang, W. Fan, Q. Yin, L. Chen, T. Cui, J. Zhang, Y. Lu, J. Cheng, P. Fu, and F. Liu. 2014. Involvement of inflammation-related miR-155 and miR-146a in diabetic nephropathy: implications for glomerular endothelial injury. BMC Nephrol. 15:142.

Hulsmans, M., D. De Keyzer, and P. Holvoet. 2011. MicroRNAs regulating oxidative stress and inflammation in relation to obesity and atherosclerosis. FASEB J. 25:2515–2527.

Jiao, S., H. Ren, Y. Li, J. Zhou, C. Duan, and L. Lu. 2013. Differential regulation of IGF-I and IGF-II gene expression in skeletal muscle cells. Mol. Cell. Biochem. 373:107–113.

Kopan, R., and M. X. G. Ilagan. 2009. The canonical Notch signaling pathway: unfolding the activation mechanism. Cell 137:216–233.

Lang, C. H., B. J. Krawiec, D. Huber, J. M. McCoy, and R. A. Frost. 2006. Sepsis and inflammatory insults downregulate IGFBP-5, but not IGFBP-4, in skeletal muscle via a TNF-dependent mechanism. Am. J. Physiol. Regul. Integr. Comp. Physiol. 290:R963–R972.

Lewis, J. R., and S. R. Mohanty. 2010. Nonalcoholic fatty liver disease: a review and update. Dig. Dis. Sci. 55:560–578.

Li, L., L. Jia, and Y. Ding. 2018. Upregulation of miR-375 inhibits human liver cancer cell growth by modulating cell proliferation and apoptosis via targeting ErbB2. Oncol. Lett. 16:3319–3326.

Liu, X.-L., Q. Pan, R.-N. Zhang, F. Shen, S.-Y. Yan, C. Sun, Z.-J. Xu, Y.-W. Chen, and J.-G. Fan. 2016. Disease-specific miR-34a as diagnostic marker of non-alcoholic steatohepatitis in a Chinese population. World J. Gastroenterol. 22:9844–9852.

Liu, A. M., R. T. P. Poon, and J. M. Luk. 2010. MicroRNA-375 targets Hippo-signaling effector YAP in liver cancer and inhibits tumor properties. Biochem. Biophys. Res. Commun. 394:623–627.

Marques-Rocha, J. L., M. Samblas, F. I. Milagro, J. Bressan, J. A. Martínez, and A. Marti. 2015. Noncoding RNAs, cytokines, and inflammation-related diseases. FASEB J. 29:3595–3611.

McCarty, R. 2017. Cross-fostering: elucidating the effects of gene-×environment interactions on phenotypic development. Neurosci. Biobehav. Rev. 73:219–254.

Panera, N., D. Gnani, A. Crudele, S. Ceccarelli, V. Nobili, and A. Alisi. 2014. MicroRNAs as controlled systems and controllers in non-alcoholic fatty liver disease. World J. Gastroenterol. 20:15079–15086.

Pirola, C. J., T. Fernández Gianotti, G. O. Castaño, P. Mallardi, J. San Martino, M. Mora Gonzalez Lopez Ledesma, D. Flichman, F. Mirshahi, A. J. Sanyal, and S. Sookoian. 2015. Circulating microRNA signature in non-alcoholic fatty liver disease: from serum non-coding RNAs to liver histology and disease pathogenesis. Gut 64:800–812.

Pogribny, I. P., A. Starlard-Davenport, V. P. Tryndyak, T. Han, S. A. Ross, I. Rusyn, and F. A. Beland. 2010. Difference in expression of hepatic microRNAs miR-29c, miR-34a, miR-155, and miR-200b is associated with strain-specific susceptibility to dietary nonalcoholic steatohepatitis in mice. Lab. Invest. 90:1437–1446.

Price, N. L., A. K. Singh, N. Rotllan, L. Goedeke, A. Wing, A. Canfrán-Duque, A. Diaz-Ruiz, E. Araldi, Á. Baldán, J.-P. Camporez, Y. Suárez, M. S. Rodeheffer, G. I. Shulman, R. de Cabo, and C. Fernández-Hernando. 2018. Genetic ablation of miR-33 increases food intake, enhances adipose tissue expansion, and promotes obesity and insulin resistance. Cell Rep. 22:2133–2145.

Rozenboim, I., J. Mahato, N. A. Cohen, and O. Tirosh. 2016. Low protein and high-energy diet: a possible natural cause of fatty liver hemorrhagic syndrome in caged White Leghorn laying hens. Poult. Sci. 95:612–621.

Salvoza, N. C., D. C. Klinzing, J. Gopez-Cervantes, and M. O. Baclig. 2016. Association of circulating serum miR-34a and miR-122 with dyslipidemia among patients with non-alcoholic fatty liver disease. PLoS One 11:e0153497.

Sayed, D., and M. Abdellatif. 2011. MicroRNAs in development and disease. Physiol. Rev. 91:827–887.

Strazzabosco, M., and L. Fabris. 2012. Notch signaling in hepatocellular carcinoma: guilty in association!. Gastroenterology 143:1430–1434.

Tan, X., R. Liu, Y. Zhang, X. Wang, J. Wang, H. Wang, G. Zhao, M. Zheng, and J. Wen. 2021. Integrated analysis of the methylome and transcriptome of chickens with fatty liver hemorrhagic syndrome. BMC Genomics 22:8.

Yamada, H., K. Suzuki, N. Ichino, Y. Ando, A. Sawada, K. Osakabe, K. Sugimoto, K. Ohashi, R. Teradaira, T. Inoue, N. Hamajima, and S. Hashimoto. 2013. Associations between circulating microRNAs (miR-21, miR-34a, miR-122 and miR-451) and non-alcoholic fatty liver. Clin. Chim. Acta 424:99–103.

Zhang, Y., Z. Liu, R. Liu, J. Wang, M. Zheng, Q. Li, H. Cui, G. Zhao, and J. Wen. 2018. Alteration of hepatic gene expression along with the inherited phenotype of acquired fatty liver in chicken. Genes (Basel) 9:E199.

Zhou, L., D.-S. Wang, Q.-J. Li, W. Sun, Y. Zhang, and K.-F. Dou. 2012. Downregulation of the Notch signaling pathway inhibits hepatocellular carcinoma cell invasion by inactivation of matrix metalloproteinase-2 and -9 and vascular endothelial growth factor. Oncol. Rep. 28:874–882.